Available online at www.sciencedirect.com
SCIENCE DIRECT®
Journal of Power Sources 144 (2005) 552–559
JOURNAL OF POWER SOURCES
www.elsevier.com/locate/jpowsour

Novel technique to ensure battery reliability in 42-V PowerNets for new-generation automobiles

L.T. Lam*, N.P. Haigh, C.G. Phyland, T.D. Huynh

CSIRO Energy Technology, Box 312, Clayton South, Vic. 3169, Australia

Abstract

The proposed 42-V PowerNet in automobiles requires the battery to provide a large number of shallow discharge–charge cycles at a high rate. High-rate discharge is necessary for engine cranking, while high-rate charge is associated with regenerative braking. The battery will therefore operate at these high rates in a partial-state-of-charge condition — 'HRPSoC duty'.

Under simulated HRPSoC duty, it is found that the valve-regulated lead–acid (VRLA) battery fails prematurely due to the progressive accumulation of lead sulfate mainly on the surfaces of the negative plates. This is because the lead sulfate layer cannot be converted efficiently back to sponge lead during charging either from the engine or from the regenerative braking. Eventually, this layer of lead sulfate develops to such extent that the effective surface area of the plate is reduced markedly and the plate can no longer deliver the high-cranking current demanded by the automobile.

The objective of this study is to develop and optimize a pulse-generation technique to minimize the development of lead sulfate layers on negative plates of VRLA batteries subjected to HRPSoC duty. The technique involves the application of sets of charging pulses of different frequency. It is found that the cycle-life performance of VRLA batteries is enhanced markedly when d.c. pulses of high frequency are used. For example, battery durability is raised from ~10 600 cycles (no pulses) to 32 000 cycles with pulses of high frequency. Two key factors contribute to this improvement. The first factor is localization of the charging current on the surfaces of the plates — the higher the frequency, the greater is the amount of current concentrated on the plate surface. This phenomenon is known as the 'skin effect' as only the outer 'skin' of the plate is effectively carrying the current. The second factor is delivery of sufficient charge to the Faradaic resistance of the plate to compensate for the energy loss to inductance and double-layer capacitance effects. The Faradaic resistance represents the electrochemical reaction, i.e., conversion of lead sulfate to lead. The inductance simply results from the connection either between the cables and the terminals of the battery or between the terminals, bus-bars, and the lugs of the plates. The capacitance arises from the double layer which exists at the interface between the plate and the electrolyte solution. These findings have provided a demonstration and a scientific explanation of the benefit of superimposed pulsed current charging in suppressing the sulfation of negative plates in VRLA batteries operated under 42-V PowerNet and hybrid electric vehicle duties.

A Novel Pulse™ device has been developed by the CSIRO. This device has the capability to be programmable to suite various applications and can be miniaturized to be encapsulated in the battery cover.

Keywords: 42-V PowerNet; Failure mode; High-rate partial-state-of-charge duty; Pulse-generation device; Hydrogen evolution; Lead–acid battery; Sulfation; Skin effect

1. Background

Within the next decade, there will be major changes in automotive technology with the introduction of several new features which will increase significantly the on-board power requirements [1]. This high power demand is beyond the capability of present 14-V alternators and thus a 42-V power network is to be adopted. In the new 'PowerNet', the battery must provide a large number of shallow discharge–charge cycles at a high rate. High-rate discharge is necessary for engine cranking, while high-rate charge is associated with

* Corresponding author.
E-mail address: lan.lam@csiro.au (L.T. Lam).

0378-7753/$ – see front matter © 2004 Elsevier B.V. All rights reserved.
doi:10.1016/j.jpowsour.2004.11.028

Fig. 1. The Novel Pulse™ device developed in the CSIRO.

regenerative braking. The battery will therefore operate at these high rates in a partial-state-of-charge condition, so called 'HRPSoC duty'. Under such duty, there is a tendency for the plates — particularly the negative plates — of valve-regulated lead–acid (VRLA) batteries to suffer from a build-up of 'hard' lead sulfate, i.e., lead sulfate which is difficult to recharge. This effect can impair battery performance and life, and can reduce charge-acceptance during regenerative braking. Moreover, the problem of over-sulfation is exacerbated during prolonged parking of the vehicle.

A pulse-generation technique has been devised in an attempt to minimize the development of hard sulfate during both HRPSoC duty and stand conditions (Fig. 1). The technique involves the application of sets of charging pulses of different frequency to the battery. The device could be powered by an integrated starter and generator (ISG), a small solar panel, or a small of supercapacitor. In the last-mentioned option, the supercapacitor is kept predominantly at a full SoC, either by the ISG or by regenerative braking during vehicle running, and is sized to provide continuous power for operation of the pulse-generation device even when the vehicle is parked for periods of several days.

2. Experimental

2.1. 42-V profile (HRPSoC Cycling)

Studies were conducted on 12-V, commercial VRLA batteries (C_{20} = 33 Ah). One cell of each battery was fitted with a Ag | Ag_2SO_4 reference electrode [2]. The batteries were then subjected to the 42-V profile shown in Fig. 2 [3–6]. The duration of the profile is short, namely, 2.35 min. The profile is composed of several current steps that simulate the power required from the battery during vehicle operation, i.e., idle–stop, cranking, power assist, engine charging, and regenerative charging. The critical steps are the cranking and regenerative charging periods. During cranking, the battery must deliver a current of 300 A for 0.5 s, i.e., a current equal to $\sim 18C_1$.

The batteries were placed in a water bath which was maintained at 40 °C. Prior to the test, the batteries were brought to a fully charged state by applying a maximum current of 2.5 A and a constant voltage of 14.7 V for a total of 24 h. The batteries were then subjected to repetitive applications of the 42-V profile. Each application was considered to be 'one cycle' and a maximum of 1200 cycles was applied. The test was terminated when the batteries could not sustain at least 960 cycles (i.e., 80% of 1200 cycles) due to decrease in the end-of-discharge voltage to the cut-off value of 9.6 V during cycling. Otherwise, the batteries were charged fully and then subjected to a further set of 1200 cycles.

2.2. Teardown analysis

After battery failure under the 42-V profile, a detailed examination was conducted to determine the distribution of lead sulfate across cross-sections of negative and positive plates in both discharged and charged states. The samples, which were taken from plates in the outermost cell below the negative terminal, were mounted in epoxy resin to allow preparation of polished cross-sections for electron probe micro-analysis (EPMA). The five remaining cells in the battery were then subjected to a full charge. After charging, samples were taken from the cell adjacent to the outermost cell and then prepared for EPMA by means of the same procedure as that used for discharged samples. Thus, obviously, samples in discharged and charged states were obtained from different plates in different cells. Data on elemental abundance were acquired with a Joel Model JXA-8900R Superprobe which was operated at an accelerating voltage of 15 kV and a nominal beam current of 50 nA. Analyses were conducted for lead, sulfur, and oxygen.

3. Results and discussion

3.1. Performance of VRLA batteries without/with pulses of low frequency

Batteries without (VR1, VR2) or with (VR3 to VR5) low-frequency pulses (0.01–0.90 kHz) during discharge and charge of the 42-V profile failed prematurely at between 10 000 and 10 650 cycles (Fig. 3). Examples of performance of VRLA batteries VR2 and VR3 under repetitive 42-V duty are given in Figs. 4 and 5. Within each set, the charge-to-discharge ratio (c:d ratio) of the battery is always low initially, but increases rapidly to a value of ~1.03. For a given set, the internal resistance of the battery increases with cycling. Furthermore, this change in internal resistance increases with the application of successive sets. For example, the internal resistance reaches ~9 mΩ in the ninth set as opposed to ~7 mΩ in the first set. The increase in internal resistance with cycling suggests a build-up of lead sulfate in the negative/positive plates which cannot be reduced/oxidized completely even during full charging.

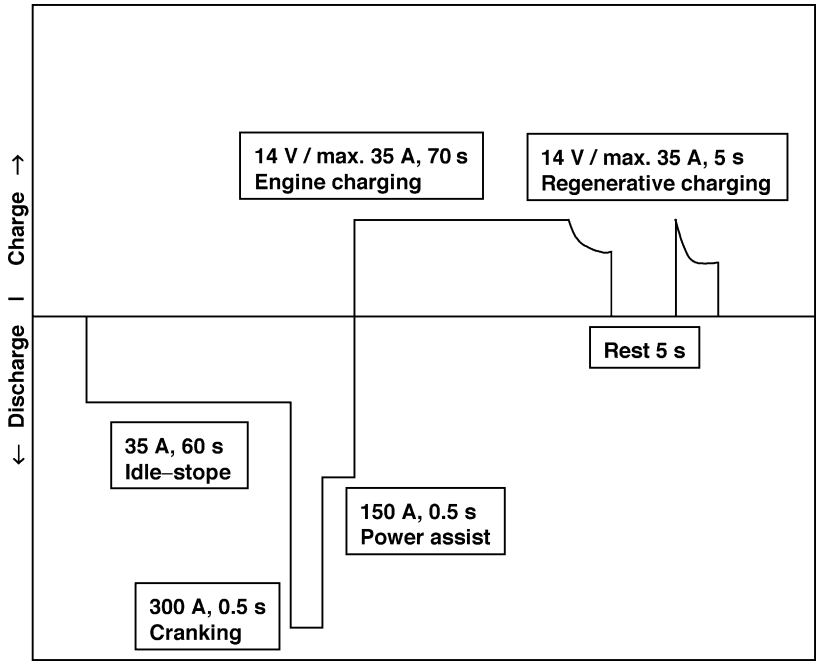

Fig. 2. The 42-V profile used for testing batteries under simulated HRPSoC.

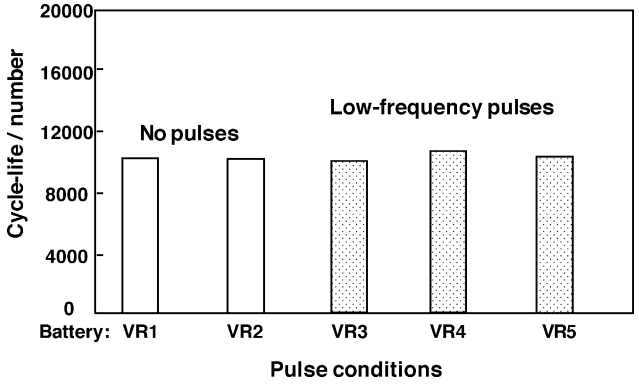

Fig. 3. Life performance of VRLA batteries under 42-V duty without and with pulses of low frequency.

The end-of-discharge voltage (EoDV) of the battery decreases slowly during individual sets of cycling and reaches the cut-off value of 9.6 V during the ninth set. On the other hand, the top-of-charge voltage (ToCV) of the battery during each set is about 14.2 V initially, but starts to increase after 30 cycles and reaches a value as high as 16.5 V. This is due to overshoot of the voltage during the early stages of the regenerative charging period. The 42-V profile includes two periods of charging: one from the engine and the other from regenerative braking (Fig. 2). Both charging procedures are regulated at a voltage of 14 V. During engine charging, the battery voltage increases and stays at 14 V. During regenerative charging, however, the battery voltage shoots rapidly above the regulated value in the early stages (i.e., <200 ms) and then decreases and remains at 14 V. Within

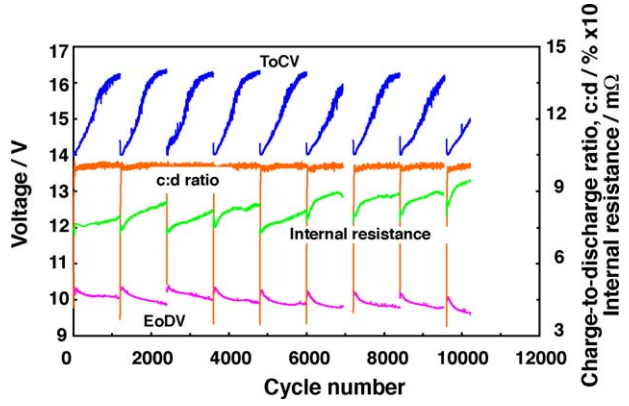

Fig. 4. Performance of VRLA battery VR2 under repetitive 42-V duty without pulses. ToCV = top-of-charge voltage; EoDV = end-of-discharge voltage.

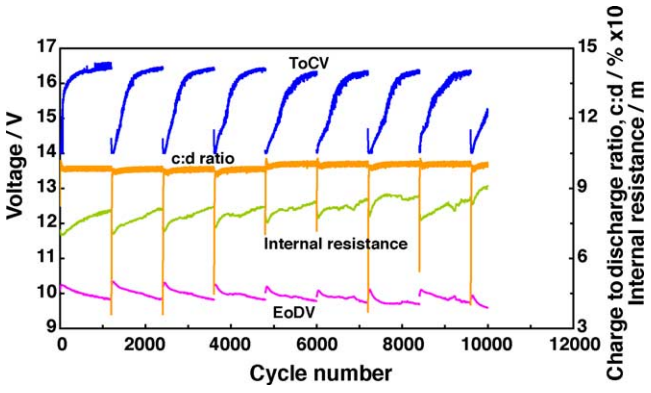

Fig. 5. Performance of VRLA battery VR3 under repetitive 42-V duty with low-frequency pulses. ToCV = top-of-charge voltage; EoDV = end-of-discharge voltage.

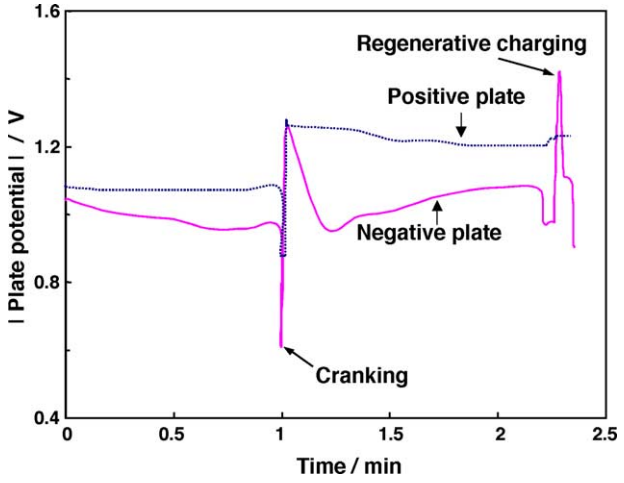

Fig. 6. Negative- and positive-plate potentials of VRLA battery VR2 during 6000th cycle of 42-V duty.

a given set, the degree of voltage overshoot increases with cycling.

It is important to determine which plate polarity is responsible for the decrease (cranking) and overshoot (regenerative charging) of the cell voltage during cycling. Changes in the negative- and positive-plate potentials during each step of the 42-V profile are shown in Fig. 6 for the 6000th cycle of battery VR2. Clearly, during engine cranking, the negative plate experiences a much greater decrease in potential than its positive counterpart. During regenerative charging, the negative-plate potential rises rapidly in the early stages of charging (i.e., <200 ms), but then decreases. This indicates that both the charge and discharge of the battery under 42-V duty is 'negative-potential limited'.

3.2. Teardown analysis

The distribution of lead sulfate across the cross-section at the central bottom of a negative plate from battery VR2, which was cycled without pulses, is shown in Fig. 7. In the discharged state (Fig. 7(a)), lead sulfate develops more on one side of the plate than on the other. Furthermore, this material concentrates on the surface of the plate, little is present in the interior. After charging, lead sulfate still remains on the surfaces of the plate and on the walls of the pores. Similar features were observed for samples taken from the central bottom of the negative plate from battery VR4 cycled with low-frequency pulses (Fig. 8). Clearly, charging is unable to convert all of the lead sulfate back to sponge lead.

The distribution of lead sulfate at the central bottom of a positive plate removed from battery VR4, which was cycled with low-frequency pulses, is shown in Fig. 9. Lead sulfate also develops mainly on the surfaces of positive plates in the discharged state, but is almost completely converted to lead dioxide after charging.

From the above observations, it can be concluded that the failure of the VRLA batteries under the 42-V profile is due to the accumulation of lead sulfate on the surfaces of the negative plates. The sulfate builds up to such extent that the plates can no longer deliver the high-cranking current required by the 42-V duty.

3.3. Mechanism of lead sulfate accumulation in negative plates under HRPSoC duty

The mechanism of lead sulfate accumulation on the surfaces of negative plates under HRPSoC duty has been documented by the authors in a previous paper [7]. The key factors responsible for such accumulation of lead sulfate are the high-rate discharge and charge. During high-rate discharging, the sponge Pb reacts with HSO_4^- to form $PbSO_4$ and this reaction proceeds so rapidly that the diffusion rate of HSO_4^- from the bulk of the solution cannot catch up with its consumption rate in the interior of negative plate. Consequently, lead sulfate forms mainly on the surface of the plate (Fig. 10). During subsequent high-rate charging, the negative-plate potential increases to such extent that, given the lower level of sulfate in the plate interior, the charging current during passage from the grid member to the plate surface reduces some hydrogen ions to hydrogen gas before reaching the lead sulfate layer (Fig. 11). Thus, complete conversion of lead sulfate at the plate surface cannot be achieved. With such repetitive action of high-rate discharge and charge, the lead sulfate will accumulate on the surfaces of negative plate and, eventually, the battery will be unable to provide sufficient power for engine cranking.

From the above discussion, it is clear that in order to improve the cycleability of VRLA batteries under HRPSoC duty, the early evolution of hydrogen should be minimized by localization of the charging current on the surfaces of the negative plate (Fig. 12). Nevertheless, the question is: How can the current be concentrated on the surface layer of the plate?

3.4. Approach to improve cycleability of VRLA batteries under HRPSoC duty

It is well known that when a direct current is passed through a conductive wire, the current will be distributed evenly throughout the entire cross-section of the wire. When, however, an alternating current (a.c.) or a direct current (d.c.) in pulsed form is passed through the same wire, the current will be localized on the perimeter of the wire. This is termed the 'skin effect' as only the outer 'skin' of the cross-section is effectively carrying the current. The penetration of the current is called the 'skin depth' and can be calculated from the following equation:

$$\text{skin depth} = \left(\frac{\rho}{\pi f \mu}\right)^{1/2} \quad (1)$$

where ρ is the bulk resistivity of the current carrier (e.g., $2.053 \times 10^{-7}\ \Omega\,\text{m}$ for lead); μ the magnetic permeability of

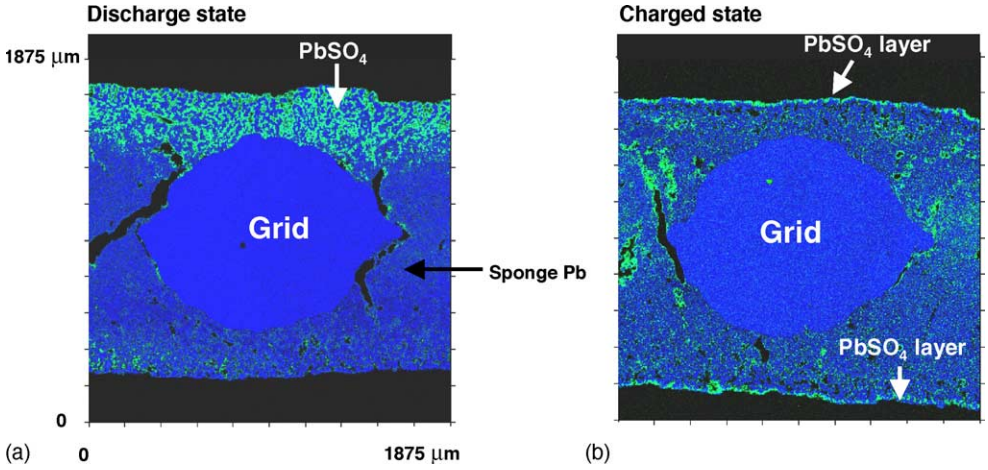

Fig. 7. Distribution of lead sulfate at central bottom of a negative plate taken from VRLA battery VR2 after failure.

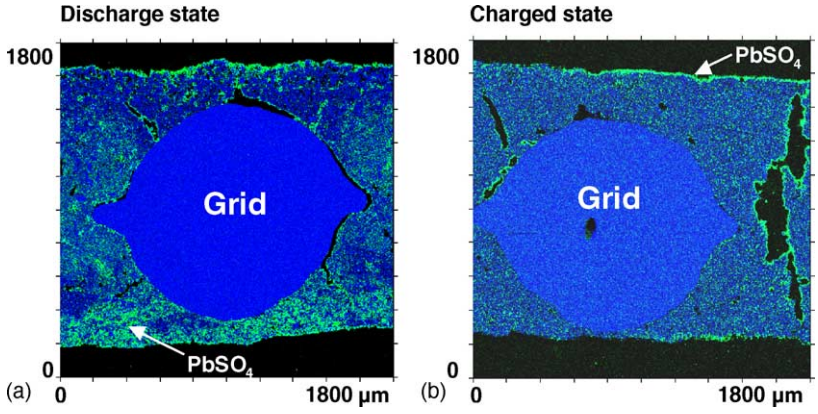

Fig. 8. Distribution of lead sulfate at central bottom of a negative plate taken from VRLA battery VR4 after failure.

free space (1.257×10^{-6} Wb (A m)$^{-1}$); f the frequency of pulsed current (Hz). In the case of a battery, the skin depth is the degree to which the current penetrates into the interior of the plate.

Eq. (1) shows clearly that the charging current will be concentrated more on the surfaces of the plate, i.e., on the lead sulfate layer, when high-frequency a.c. and/or d.c. pulses is/are used. With this knowledge, the pulse devices were redesigned to provide d.c. pulses of medium (i.e., 1–40 kHz) and high frequencies (i.e., 50–500 kHz) and a.c. 'ring' pulses of 1–5 MHz. The latter pulses could also be combined with low-frequency or medium-frequency d.c. pulses and operated only during the on-time of the d.c. pulses. Accordingly, several VRLA batteries were prepared and subjected to the

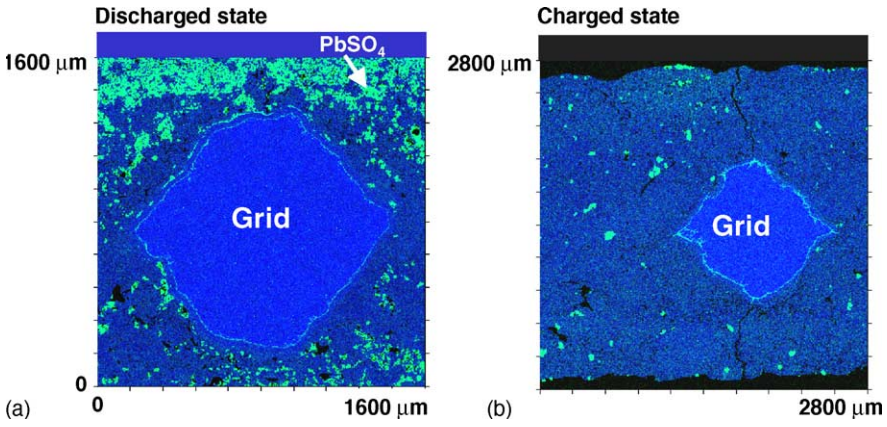

Fig. 9. Distribution of lead sulfate at central bottom of a positive plate taken from VRLA battery VR4 after failure.

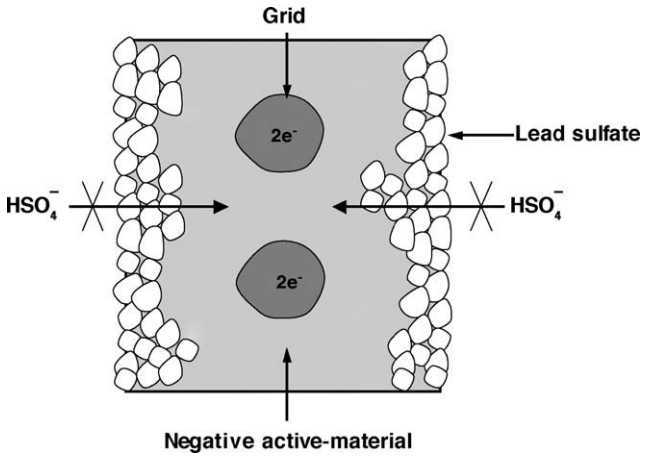

Fig. 10. Schematic representation of the distribution of lead sulfate in a negative plate subjected to high-rate discharge.

same test conditions as for batteries VR1 to VR5. These batteries were superimposed with combined a.c. 'ring' and low-/medium-frequency pulses (VR6 to VR8) or only medium-frequency pulses (VR9).

3.5. Performance of VRLA batteries with combined a.c. 'ring' and d.c. pulses of medium frequency

The performance of VRLA batteries with either combined a.c. 'ring' and d.c. pulses of medium frequency or only medium-frequency pulses is superior (15 000–18 800 cycles) to that of batteries without/with low-frequency pulses (10 000–10 650 cycles), see Fig. 13. Although these batteries still failed because of negative-plate sulfation, build-up of lead sulfate occurred throughout the entire cross-section of the plate rather than predominantly on the surface as found in batteries without/with low-frequency pulses [5]. This indicates that the use of either combined a.c. 'ring' and d.c. pulses or only medium-frequency d.c. pulses has assisted the charging of lead sulfate on the plate surface, and has allowed the discharge process to penetrate deep into the interior of the plate. Thus, the performance of the batteries is enhanced.

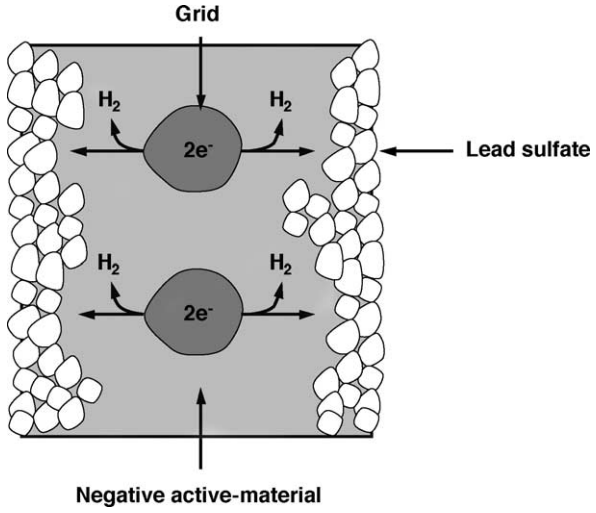

Fig. 11. Schematic representation of the charging process of a negative plate after high-rate discharge.

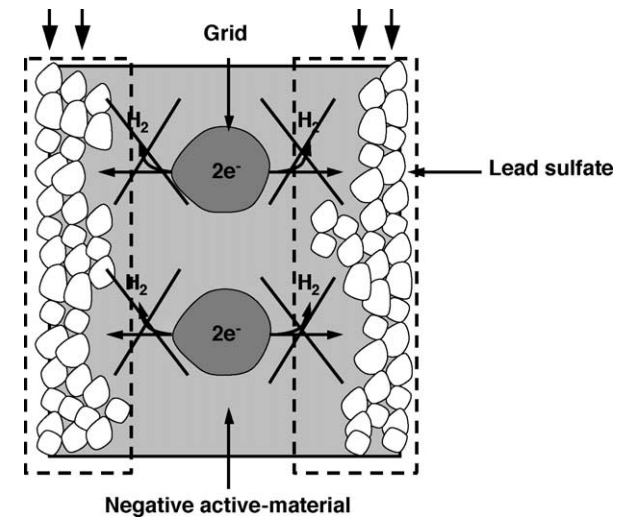

Fig. 12. A way to minimize the hydrogen evolution by localization of charging current on the surface layer of the negative plate.

3.6. Performance of VRLA batteries with d.c. pulses of high frequency

Given the above encouraging results, the following tests were conducted to optimize only the d.c. pulses, but with the high frequency (50–500 kHz) technique because this technique is easier to control than the a.c. 'ring' alternative. Accordingly, battery VR10 was prepared and subjected to the 42-V profile. It is clear that the battery VR10, superimposition of pulses with high frequency, gives a further, and remarkable, increase in cycle-life, namely, 32 000 cycles (Fig. 14). The improvement is three times that of batteries without or with low-frequency pulses. To date, these tests were conducted on commercial VRLA batteries having the 10-h capacity of

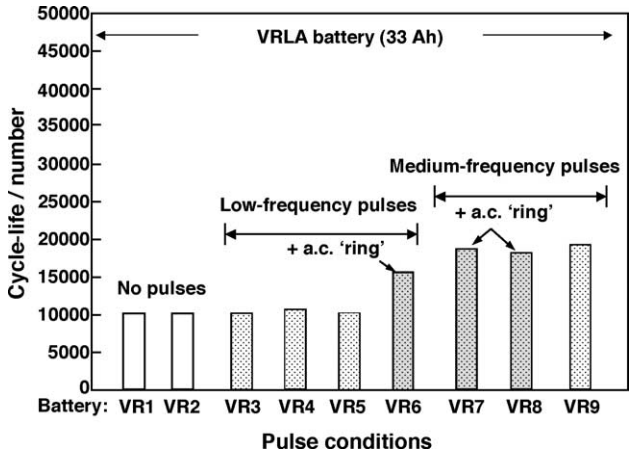

Fig. 13. Life performance of batteries operated without and with pulses.

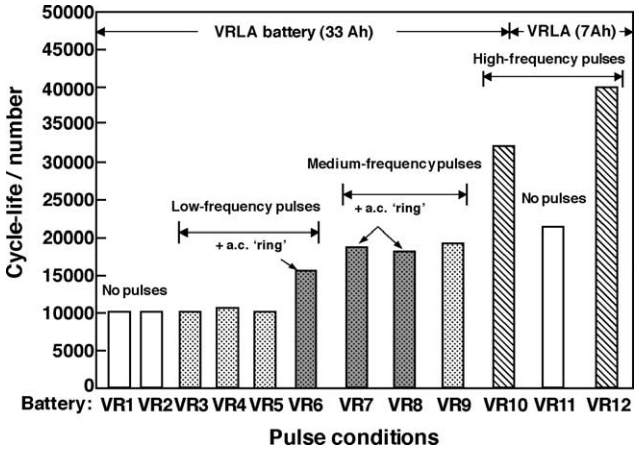

Fig. 14. Life performance of batteries operated without and with pulses.

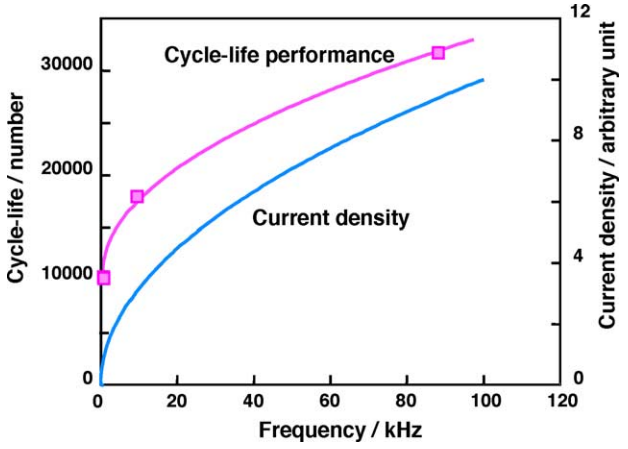

Fig. 15. Change in cycle-life performance of VRLA batteries and pulsed current density with frequency.

33 Ah. In order to reconfirm the benefits of the high-frequency pulses, the next step is to repeat the test, but on a smaller commercial VRLA battery. Two 7-Ah, VRLA batteries (VR11 and VR12) were prepared and subjected to the 42-V profile. This profile is similar to that used to test the 33 Ah batteries, except that current amplitudes during idle–stop, cranking, power assist, engine charging and regenerative charging are scaled down to 7, 60, 30, 7 and 7 A, correspondingly. Furthermore, in the interests of expediency, the battery was subjected repetitively to this profile at 40 °C until the battery voltage reached 7.2 V. The battery without pulses achieves about 20 000 cycles, while the battery with high-frequency pulses achieves about 42 000 cycles (Fig. 14). This clearly indicates again that high-frequency pulses improve the life of VRLA batteries.

To date, the above results have demonstrated that the cycle-life of VRLA batteries under HRPSoC duty can be improved substantially by the superimposition of d.c. pulses of high frequency. This improvement is considered to be the consequence of more charging current being concentrated on the surfaces of the negative plate via the skin effect. This hypothesis can be tested by making a simple comparison between the trends in pulsed current density with frequency and battery cycle-life with pulse frequency. The pulsed current density is proportional to the reciprocal of the skin depth and, therefore, is proportional to the square root of frequency, i.e.,

$$i_p \propto \frac{1}{(\rho/\pi f \mu)^{1/2}} \propto f^{1/2} \quad (2)$$

This relationship is shown in Fig. 15, together with the cycle-life performance of batteries superimposed with only d.c. pulses as a function of frequency. Clearly, the two curves follow similar trend with frequency and this indicates that the improved cycle-life of the VRLA batteries is due to concentration of the charging current on the surfaces of the negative plates.

4. Conclusions

Electron probe micro-analyses demonstrate that the failure of VRLA batteries under HRPSoC duty is due to the progressive accumulation of lead sulfate on the surfaces of the negative plates. The lead sulfate is difficult to convert back to sponge lead during charging without or with the superimposition of d.c. pulses of low frequency. This is because, given the lower level of sulfate in the plate interior, the charging current during passage from the grid member to the plate surface reduces hydrogen ions to hydrogen gas before reaching the lead sulfate layer. Thus, complete conversion of lead sulfate at the plate surface cannot be achieved, even with an overcharge of 10%.

We propose that the lead sulfate layer can be 'charged' by localizing the current on the surface of the plate via the use of d.c. pulses of high frequency — the higher the frequency, the greater is the concentration of current on the plate surfaces. This is known as the skin effect. Accordingly, the cycle-life performance of VRLA batteries is enhanced significantly when d.c. pulses of high frequency are used (i.e., 10 600 cycles (no pulses) versus 32 000 cycles (with pulses of high frequency)). Nevertheless, when the high-frequency pulses are applied to the battery, there will be some energy loss to inductance and the double-layer capacitance effect. The inductance is simply caused by the metallic connection either between the cable and the battery or between the terminals, bus-bar and plate lugs. The capacitance is developed by the double layer at the interface between the plate and the electrolyte solution. Thus, the pulse conditions should be chosen so that it can provide sufficient charge to convert the lead sulfate layer. The Novel Pulse^{TM} device developed at the CSIRO has been covered by United States Provisional Patent application [8] and a subsequent International Patent application [9]. This device has the features and benefits of: (i) programmable to suite to applications; (ii) superior performance so it can give longer battery life; (iii) reconfigurable

for a wide range of applications; (iv) miniaturization to be encapsulated in battery cover.

Acknowledgement

This work has been supported by the Advanced Lead–Acid Battery Consortium, Research Triangle Park, NC, USA.

References

[1] K. Peters, M.G. Mayer, D.A.J. Rand, Proceedings of the Fourth International Conference and Exhibition: Vehicle Electronic Systems 2001, Coventry, UK, 27–28 June 2001, ERA Report 2001-0214, Project 400059925, Paper 9.2, pp. 9.2.1–9.2.11.
[2] P. Ruetschi, J. Power Sources 116 (2003) 53–60.
[3] T. Noda, K. Hata, K. Yamanaka, K. Yamaguchi, M. Tsubota, Paper Presented at the Ninth Asian Battery Conference, Bali, Indonesia, September, 2001.
[4] L.T. Lam, C.G. Phyland, D.A.J. Rand, A.J. Urban, Novel technique to ensure battery reliability in 42-V powernets for new-generation automobiles, ALABC Project C 2.0, Progress Report, August 2001–January 2002, CSIRO Energy Technology, Investigation Report ET/IR480R, March 2002, 19 pp.
[5] L.T. Lam, N.P. Haigh, C.G. Phyland, D.A.J. Rand, A.J. Urban, Novel technique to ensure battery reliability in 42-V powernets for new-generation automobiles, ALABC Project C 2.0, Final Report, August 2001–November 2002, CSIRO Energy Technology, Investigation Report ET/IR561R, December 2002, 39 pp.
[6] L.T. Lam, N.P. Haigh, C.G. Phyland, T.D. Huynh, D.A.J. Rand, Novel technique to ensure battery reliability in 42-V powernets for new-generation automobiles, ALABC Project C 2.0, Extended Report, January–April 2003, CSIRO Energy Technology, Investigation Report ET/IR604R, May 2003, 23 pp.
[7] L.T. Lam, N.P. Haigh, C.G. Phyland, A.J. Urban, J. Power Sources 133 (2004) 126–134.
[8] United States Patent Application No. 60/444559.
[9] International Patent Application No. PCT/AU2004/0001221.